Experimental Study on Remote Manipulation Using Virtual Reality

Eimei Oyama and Naoki Tsunemoto
Mechanical Engineering Laboratory
Namiki 1-2, Tsukuba Science City
Ibaraki 305, Japan

Susumu Tachi
RCAST, The University of Tokyo
Komaba 4-6-1, Meguro
Tokyo 153, Japan

Yasuyuki Inoue
Tsukuba Research Center, Yasukawa Electric Manufacturing Corp.
Tohkohdai 5-9-10, Tsukuba Science City
Ibaraki 305, Japan

Abstract

To control a slave robot in poor visibility environments, an experimental extended tele-existence system using virtual reality was constructed. The environment model was constructed from the design data of the real environment. When virtual reality is used for controlling a slave robot, the modeling errors of the environment model must be calibrated. A model-based calibration system using image measurements is proposed for matching the real environment and the virtual environment. The slave robot has an impedance control system for contact tasks and for compensating for the errors that remain after the calibration. After the calibration, an experimental operation in a poor visibility environment was successfully conducted.

1 Introduction

Tele-existence is an advanced type of teleoperation system that enables a human operator to perform remote manipulation tasks dexterously with the feeling that he or she exists in the remote anthropomorphic robot operating in a remote environment (Tachi, Tanie, & Komoriya, 1981; Tachi & Abe, 1982; Tachi, Tanie, Komoriya, & Kaneko, 1984). This is similar to telepresence (Akin, Minsky, Thiel, & Kurtman, 1983).

Much effort has been made to develop tele-existence or telepresence (Tachi & Arai, 1985; Hightower, Spain, & Bowles 1987; Stark et al., 1987; Tachi, Arai, & Maeda, 1990). Recently, virtual reality technology, one of the origins of which is telepresence or tele-existence, has become popular through the rapid increase of the performance of graphics computers and by the development of new convenient devices such as the data glove and the lightweight head-mounted stereo display (Fisher, McGreevy, Humphries, & Roinett, 1986).

Supervisory control using the virtual environment generated by computer graphics was proposed and developed for the remote robot control (Sheridan, 1982; Noyes & Sheridan, 1984; Hashimoto & Sheridan 1986; Bejczy & Kim, 1990; Bejczy, Kim, & Venema, 1990; Machida, Toda, & Iwata, 1990; Park & Sheridan, 1991).

The extended tele-existence system using virtual reality technology for the extension of human functions has been proposed (Tachi, Arai, & Maeda, 1988). This system provides supervisory control using a virtual environment which mimics the real situation. For instance, in smoke filled environments, environmental information is almost invisible to humans. However, visual information about the environment can be generated with computer graphics from the environment model and a virtual environment with the real-time sensation of presence can be constructed. The operator can work in the visible vir-

Presence, Vol. 2, No. 2, Spring 1993, 112–124

tual environment with the feeling that he or she is in a visible real environment. The slave robot can work in the nearly invisible real environment. To operate a slave robot in poor visibility environments, an experimental study of the remote manipulation using virtual reality is presented. The experimental extended tele-existence system was constructed.

Using the virtual environment to control a slave robot, the modeling errors of the environment model become critical. The environment model used in the virtual environment has been constructed from the design data of the environment. However, there are usually errors in the environment model. In particular, a contact task is difficult when the virtual environment does not accurately correspond to the real environment. A method for adjusting the parameters of the environment model using image measurement is presented as an environment model calibration system. The slave robot in the experimental system has only a stereo video camera as its external sensor. Since measurements cannot be taken during operation in nearly invisible environments, this system has only limited performance. However, if the robot has a range sensor that can work in such nearly invisible environments, the proposed method can be applied to real-time model error correction during operation.

Even if there has been successful calibration, the safe control of the slave robot still cannot be performed with the position control when undertaking a contact task. Even small errors that remain after the calibration may make the robot arm unstable. However, impedance control stabilizes the slave robot arm even during contact tasks involving hard objects (Hogan, 1985, 1987; Inoue, Tachi, & Arai, 1992). An experimental operation in a poor visibility environment was successfully conducted.

2 Extended Tele-existence System

This section discusses the tele-existence system extended with a virtual reality system.

2.1 Extended Tele-existence System with Virtual Reality

During our research on tele-existence, the extension of human functions using the artificial or virtual reality technology was proposed (Tachi et al., 1988). The incorporation of a virtual environment simulator in a tele-existence system and the improvement of the intelligence of a slave robot can extend human functions.

The use of an environment simulator enables the training of a task, which facilitates the execution of a task in the real world. If the virtual environment adequately corresponds to the real environment, a slave robot can be operated in a poor visibility real environment through a human operator working in a matched virtual environment.

Figure 1 shows the conceptual diagram of the extended tele-existence system. The extended tele-existence system includes an environment simulator and an environment model manager. The environment simulator simulates the working environment of the robot and constructs the virtual environment. A human operator can work in the virtual environment with the feeling that he or she is working in the real environment.

The environment model manager continuously corrects the environment model by using the sensory information from the slave robot. In the conventional tele-existence system, the operator is directly connected to the slave robot, while he or she is indirectly connected to the slave robot in the extended tele-existence system. The virtual environment between the operator and the slave robot is based on the real environment and it can be integrated with various kinds of information that are useful for different operations.

2.2 Experimental Extended Tele-existence System

To test the effectiveness of robot control by tele-existence, we constructed an experimental tele-existence system (Tachi et al., 1990). Working towards the extended tele-existence system shown in Figure 1, we incorporated a virtual reality system into the tele-existence system and constructed an experimental extended tele-

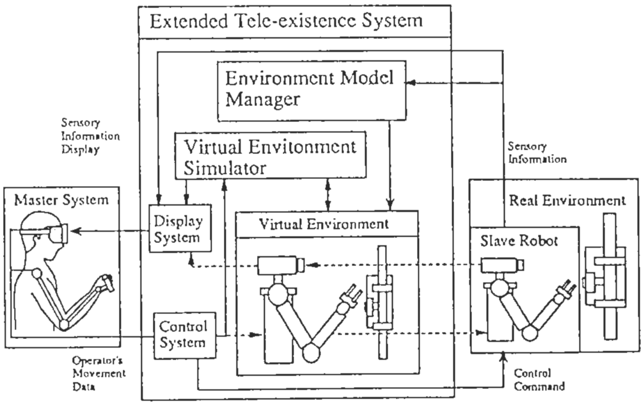

Figure 1. *Extended tele-existence system with virtual reality.*

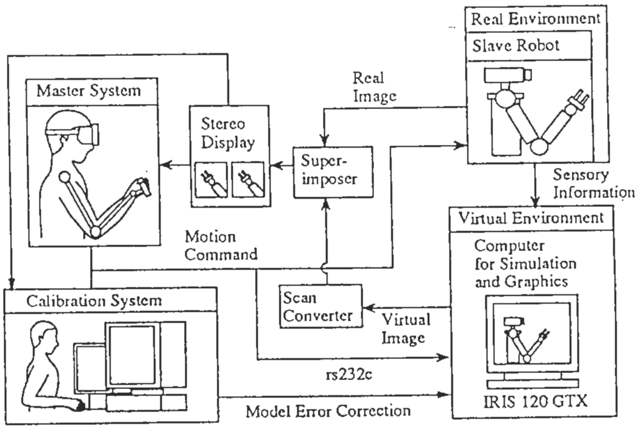

Figure 2. *Configuration of experimental extended tele-existence system.*

existence system as shown in Figure 2 (Tachi, Arai, Maeda, Oyama, Tsunemoto, & Inoue, 1991). Subsystems will be described in subsequent sections. Although the environment model manager has not been fully implemented, some of its functions have been installed in the calibration system, which will be discussed in the next section.

2.3 Master System

Figure 3 shows a view of the tele-existence master system. The audio-visual display is carried by a link mechanism with 6 degrees of freedom (DOF). The link mechanism, which can measure the three-dimensional orientation of the operator's head by using three rotary encoders, cancels all gravitational force through a counterbalancing mechanism. Therefore the operator feels only inertial forces. Stereo visual display is designed according to an established procedure (Tachi et al., 1984) that ensures that the three-dimensional view will maintain the same spatial relation as that resulting from direct observation.

The master system has a 7 DOF master arm. The structural dimensions of the master arm are the same as those of the slave arm and are set very close to those of a human arm. The master arm measures the movement of the operator's arm by using seven rotary encoders. The master system measures the movement of the operator and sends it to the slave system and the virtual reality system.

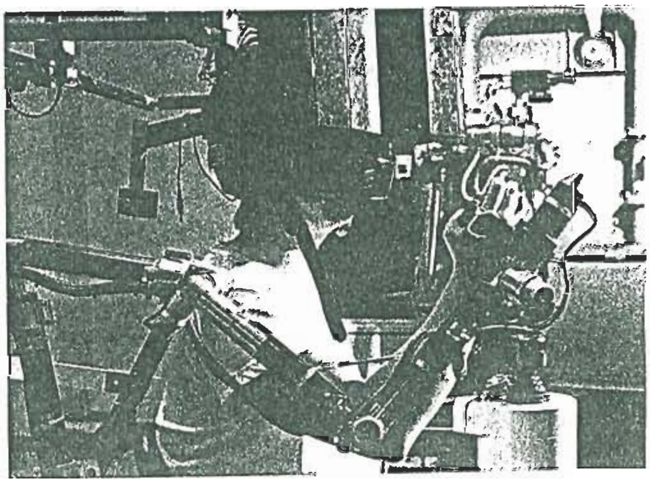

Figure 3. *Master system.*

This master system does not have a force feedback system. So the master–slave operation is conducted by unilateral control. The force feedback system is presently under development.

2.4 Slave System

Figure 4 shows a view of the anthropomorphic slave robot in the experimental tele-existence system. The robot's structural dimensions were set very close to those of a human (Tachi et al., 1990). The slave robot

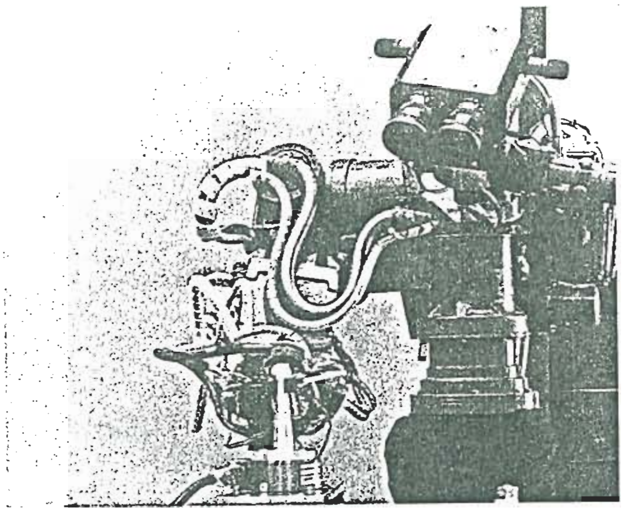

Figure 4. *Slave system.*

has a 3 DOF neck mechanism on which a stereo camera is mounted, an arm with 7 DOF, and a torso mechanism with 1 DOF. The arm can carry a 1 kg load at the maximum speed of 3 m/sec. The slave arm has a 6 DOF force sensor on the wrist joint. The impedance control (Hogan, 1985, 1987) is applied for the control of the arm to perform contact tasks as described in the following section. The position of the slave robot, which can move on a horizontal plane, is controlled with a joy stick and foot switch by the operator.

2.5 Impedance Control

When the robot tries to perform contact tasks or when its arm collides with an unexpected object, the arm becomes unstable by position feedback control. It may break the object or it may break itself. To solve this problem, impedance control was proposed and developed for the contact tasks (Hogan, 1985, 1987; Tachi & Sakaki, 1990).

Let the position of the endpoint of the robot arm be x, the reference point be x_r and the difference vector between x and x_r be e expressed as:

$$e = x - x_r \tag{1}$$

Impedance control tries to control x to attain the desired mechanical impedance characteristics according to the external force that affects the robot hand. The impedance characteristics including inertia, viscosity, and elasticity is expressed as:

$$M\ddot{e} + B\dot{e} + Ke = F \tag{2}$$

where M is the inertia factor matrix, B is the viscosity factor matrix, K is the elasticity factor matrix, and F is the external force vector, respectively. When M and B are set to 0, this control is called compliance control (Mason, 1981; Salisbury, 1980; Bejczy & Kim, 1990).

We applied the impedance control to the master–slave manipulation (Tachi et al., 1991; Inoue et al., 1992). In our system, the impedance control is conducted as follows. For the master slave manipulation, x is the position of the endpoint of the slave arm x_s and the reference position x_r is the position of the endpoint of master arm x_m, i.e.,

$$x = x_s \tag{3}$$

$$x_r = x_m \tag{4}$$

Let the joint angle vector of the master arm be θ_m and the joint angle vector of the slave arm be θ_s. x_s and x_m can be calculated by using the kinematics models $f(\theta)$, i.e.,

$$x_s = f(\theta_s) \tag{5}$$

$$x_m = f(\theta_m) \tag{6}$$

According to Eq. (2), e is calculated by using the data from the force sensor on the wrist joint of the slave arm. Hence the desired joint angle vector of the slave arm calculated by the following equation:

$$\theta_s = \theta_m + J^*(\theta)e$$

$$J(\theta) = \frac{\partial f(\theta)}{\partial \theta} \tag{7}$$

$$J^*(\theta) = J^T(\theta)[J(\theta)J^T(\theta)]^{-1}$$

where J^T is the transpose of J. The servo controller for the motors can achieve this desired joint angle vector. Impedance control allows the slave robot arm to remain stable during contact tasks involving hard objects (Tachi et al., 1991; Inoue et al., 1992).

2.6 Virtual Reality System

The virtual reality system consists of one graphics computer, two scan converters, and two superimposers. The graphics computer, the IRIS 120 GTX shown in Figure 2, receives the data of the operator's movement from the master system through a desktop computer. It updates the virtual environment by using simplified physical laws to simulate the real environment. It then displays the virtual environment on its screen. For instance, a picture of the training of block stacking is shown in Figure 5. In the display system, both left and right images are displayed on the graphics computer screen. The images are split by the scan converters and are sent to the stereo display system. The real image from the slave robot and the virtual image created by the computer can be interchanged or overlaid on the display by the superimposer. This function is essential for controlling a robot using virtual reality and the calibration of the environment model by using images. The position of a point on the real images can be measured by overlaying the mouse cursor of the graphics computer on the real image. Figure 6 shows the virtual image displayed on a monitor screen and on a computer graphics display.

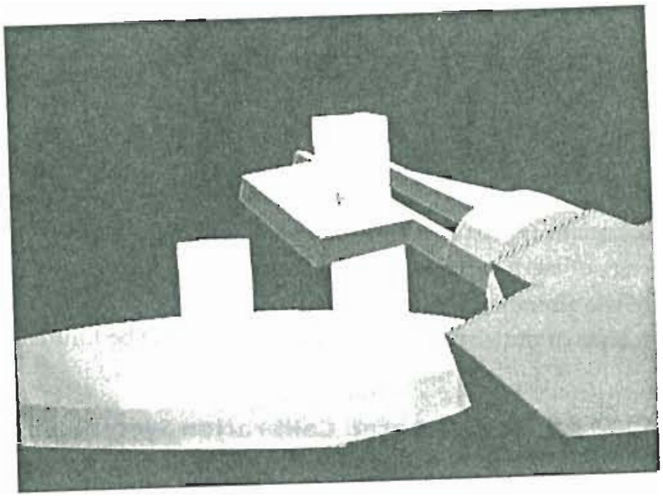

Figure 5. *Training of block stacking.*

Figure 6. *Virtual image on graphics computer display.*

3 Model-Based Calibration System

This section describes the calibration system in the extended tele-existence system.

3.1 Modeling Error Problem

There are usually some errors in the environment model. Large errors may cause the operation to fail in a nearly invisible environment. To reduce such errors, the extended teleexistence system should continuously calibrate the environment model by using sensory information from the external sensors of the slave robot.

The environment model in the virtual reality system is usually described by the symbolic structural description of the model and the values of the parameters in the description. The parameters specify the shapes and the movement of objects. For example, let us consider a lever rotating about its axis by changing its rotation angle. The position and the orientation of the lever based on a given coordinate can be obtained by using some measurement techniques. However, such information is not useful for virtual reality simulations. The measured data must be transformed to the rotational angle. Therefore measurements based on the description of the environment model must be conducted.

Another kind of error is the structural error within the environment model (e.g., the error that occurs when a cube is modeled by a cone). This type of error may be more important in practical operations. In cases such as the outbreak of fire, where shapes are completely changed, it would probably be impossible to achieve an adequate approximation simply by adjusting the parameters of environment models. In such cases the function of the altered object is also changed, and the performance of the virtual environment system will be limited.

3.2 Model-Based Calibration System

ACRONYM system, one of the first model-based vision systems, has object models described by a kind of model description language with a set of parameter values. It tries to estimate the values of the unknown parameters that determine the viewpoint of the scene by symbolic reasoning (Brooks, 1981). However, the image measurement equation that represents the relationship between the positions of the points of an object on the image and the viewpoint is too difficult for symbolic reasoning. Therefore, the use of the nonlinear least-squares method to solve the image measurement equation was proposed and developed (Lowe, 1980, 1985, 1987; Tanabe, Ohyama, & Koyama, 1985, 1986; Gunnarsson & Prinz, 1987). It was also suggested that the internal parameters of the objects can be estimated using numerical differentiation (Lowe, 1987).

Based on this idea, we have developed a generalized measurement system for calibrating the environment model. This system formulates the measurement equation from the object model and the definition of the measurement model. The object model is described by a kind of model description language and the measurement model can be defined by measurement model description language or a set of subroutines that calculates the values of the measurement model. This system uses the nonlinear least-squares method to estimate the unknown parameters for the descriptions of objects (Oyama & Tachi, 1990).

By using the numerical method and the random search techniques of the initial values of the estimated parameters, any parameter that has observability in the measurement equation can be estimated. Therefore the proposed measurement system is well suited for the calibration of the environment model. For this reason, we have incorporated the proposed system into the extended tele-existence system after slight modifications.

3.3 Configuration of the Measurement System

Let the known parameter vector be p, the unknown parameter vector be x, and the measurement model be $h(p, x)$. The measurement vector y is the sum of the true measurement model $h(p, x)$ and the noise vector ω. The measurement equation can be defined as follows.

$$y = h(p, x) + \omega \tag{8}$$

We assume that ω, the noise vector, is Gaussian. The weight matrix W is the inverse matrix of the covariance matrix of ω, i.e.

$$W = E(\omega\omega^T)^{-1} \tag{9}$$

where $E(A)$ is the average of a matrix A.

$$S = [y - h(p, x)]^T W [y - h(p, x)] \tag{10}$$

This problem can be solved by randomly searching for the initial value of x and by using the nonlinear least-squares methods such as Marquardt's method (Marquardt, 1963) (see Section 3.4). Therefore, the acquisition of the measurement vector y and the calculation of the value of $h(p, x)$ become the main problems in making the estimation.

E_r represents the real environment. The measurement vector y can be obtained by using the measurement value acquisition function $meas_r(E_r)$, i.e.

$$y = meas_r(E_r) \tag{11}$$

By making $meas_r(E_r)$ and evaluating it, the measurement vector can be obtained. D represents the description of the environment model using unknown parameters and X represents the values of these parameters. Some components of X correspond to unknown parameter vector x while other components correspond to known parameter vector p. X can be calculated using the parameter vector conversion function $param(p, x)$, which can be expressed as:

$$X = param(p, x) \tag{12}$$

E_v represents the virtual environment that consists of the solid or the surface models of the objects. For some kinds of measurement values, the measurement model $h(p, x)$ can be directly extracted from the description of the environment model D. However, there are many kinds of measurement values such as range data that cannot easily be extracted from D. Therefore the measurement model $h(p, x)$ is calculated from the 3-D modeler program generating the virtual environment in the virtual reality system. $Modeler(D, X)$ represents the 3-D modeler that converts D to E_v expressed as:

$$E_v = modeler(D, X) \tag{13}$$

The measurement model $h(p, x)$ is calculated by using the measurement value extraction function $meas_v(E_v)$, which derives the measurement values from the virtual environment E_v. Then $h(p, x)$ can be calculated as

$$h(p, x) = meas_v(modeler(D, param(p, x))) \tag{14}$$

The main problem for the user to solve is to make $meas_v(E_v)$. Fortunately it is not difficult. The measurement system already has many functions that derive various measurement values from the virtual environment.

The model-based calibration system consists of the following modules (see Fig. 7).

1. Human interface: The operator selects the kinds of measurement values and the parameters to be estimated through this module. This module defines x, p and $param\ (p, x)$.
2. The measurement value acquisition module: This module, which conducts the measurement and creates the measurement vector, corresponds to $meas_r(E_r)$.
3. The virtual environment generator: This module creates the virtual environment from the description of the environment model. The program is the same as the 3-D modeler that generates the virtual environment. This module corresponds to $modeler\ (D, X)$.
4. The measurement model calculator: This module, which calculates the value of the measurement model from the virtual environment, corresponds to $meas_v(E_v)$.
5. The measurement equation solving module: This module solves the measurement equation by using the nonlinear least-squares methods.

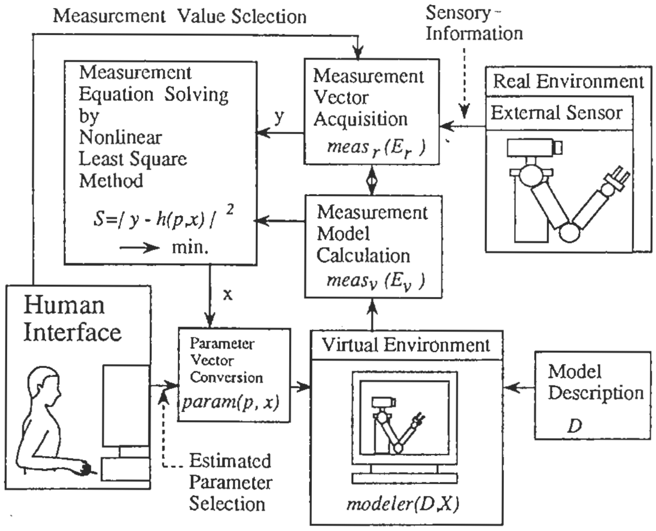

Figure 7. *Configuration of model-based calibration system.*

3.4 Method for Estimating Unknown Parameters

Marquardt's method (Marquardt, 1963) is used for minimizing the evaluation function S in Eq. (10). When k is the number of iterations, this method improves the estimated value $x(k)$ iteratively as follows:

$$x(k + 1) = x(k) + \Delta x(k) \tag{15}$$

$$\Delta x(k) = K(p, x(k))(y - h(p, x(k))) \tag{16}$$

$$K(p, x) = [H(p, x)^T W H(p, x) + \lambda I]^{-1} H(p, x)^T W \tag{17}$$

$$H(p, x) = \frac{\partial h(p, x)}{\partial x} \tag{18}$$

$H(p, x)$ is the Jacobian of the measurement model $h(p, x)$. λ is a nonnegative parameter adjusted to suit the degree of nonlinearity. If there is observability of the measurement Eq. (8), $x(k)$ converges to a correct solution by randomly searching the initial value of the unknown parameter vector $x(0)$. Though the Marquardt's method requires the Jacobian of the measurement model, the Jacobian can be easily obtained through numerical differentiation.

Most nonlinear systems become almost linear at the point of convergence. At this stage, λ should become

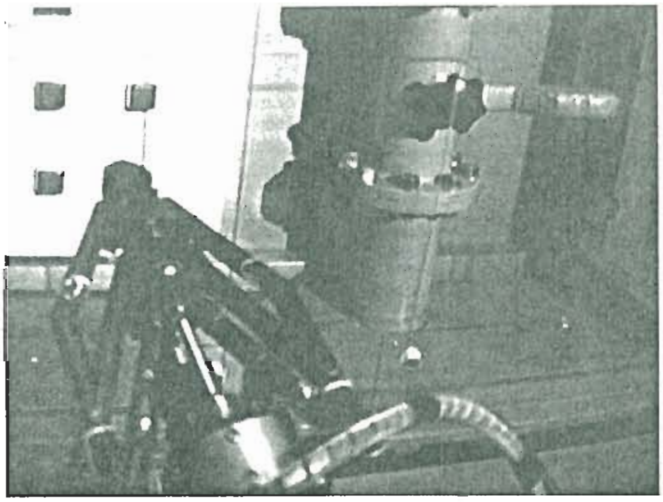

Figure 8. *Tele-existence experimental environment.*

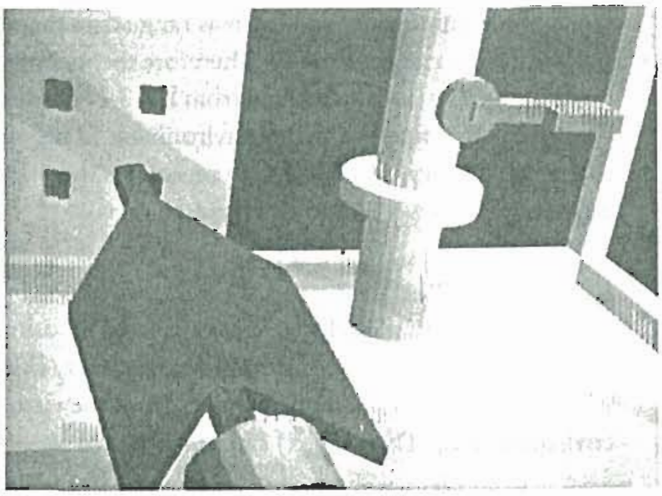

Figure 9. *Environment model.*

zero. If λ is zero and $K(p, x)$ cannot be calculated due to the numerical instability of Eq. (17), there is no observability in the equations and the true value of the parameter vector cannot be obtained. In such instances, the measurement vector or the estimated parameter vector will need to be checked or the acquisition of additional measurement values will be required.

3.5 Image Measurement

Since the stereo camera is the slave robot's only external sensor, we constructed the calibration system using images from the slave robot. This calibration requires the help of a human operator to obtain the measurement vector y from the images. However, if the slave robot has a range sensor, an operator is not necessary and automatic calibration can be performed.

This measurement system calculates the value of the measurement model $h(p, x)$ using the screen drawing procedure. It can also solve the least-squares minimization problem by Marquardt's method and estimates unknown parameters.

Mapping positions of points on an object to points on a camera image are subject to rotational, translational, and perspective transformations. Using the positions of points on the screen as measurement values, the measurement model can be derived by making various transformations on the base vectors [e.g., $(1,1,1)^T$ in 3-D space]. A computer graphics system generating a virtual environment has procedures that can transform the basic vectors to the points on the screen. The numerical values of the positions of the points can easily be obtained by using the screen drawing and painting procedure in computer graphics.

When formulating the measurement equation, a point on the screen and a point on the object must correspond to each other. The measurement equation can be formulated with the assistance of an operator using a mouse to select points of objects in the virtual image and the corresponding points in the real image on the screen. This procedure is nearly identical to the camera calibration system proposed in Bejczy et al. (1990). After the selection of these points, they are digitized.

After calculating the least-squares method using several initial values, the solution vector with the smallest residual is selected. If the estimation fails, the measurement procedure has to be repeated to obtain sufficient observations.

4 Experiment

We conducted some experiments with the calibration method and a test operation in a nearly invisible environment.

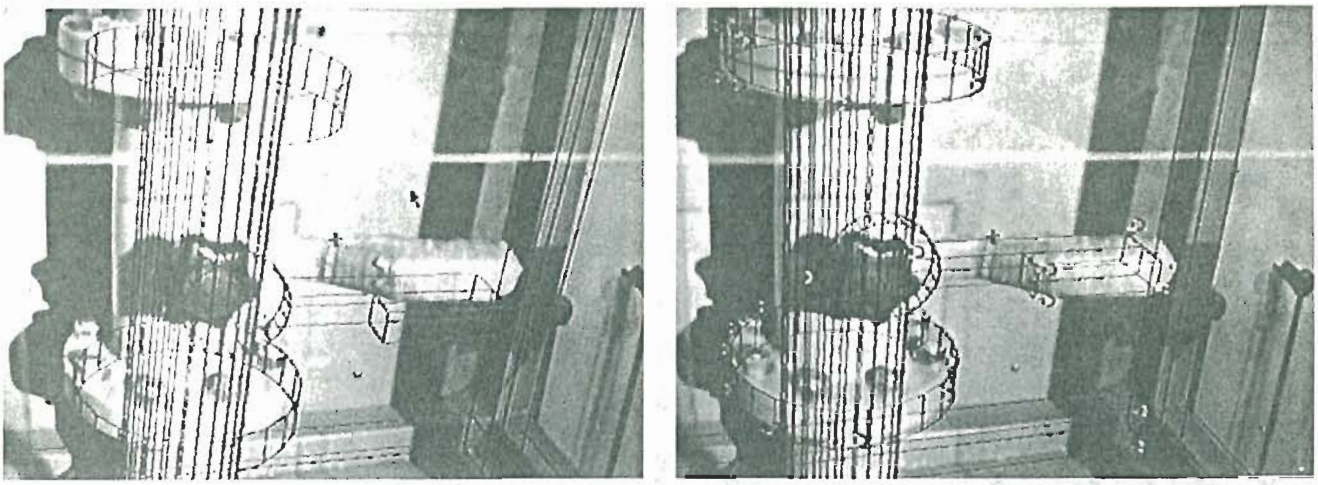

Figure 10. *Superimposed images during calibration. (a) Before calibration. (b) After calibration.*

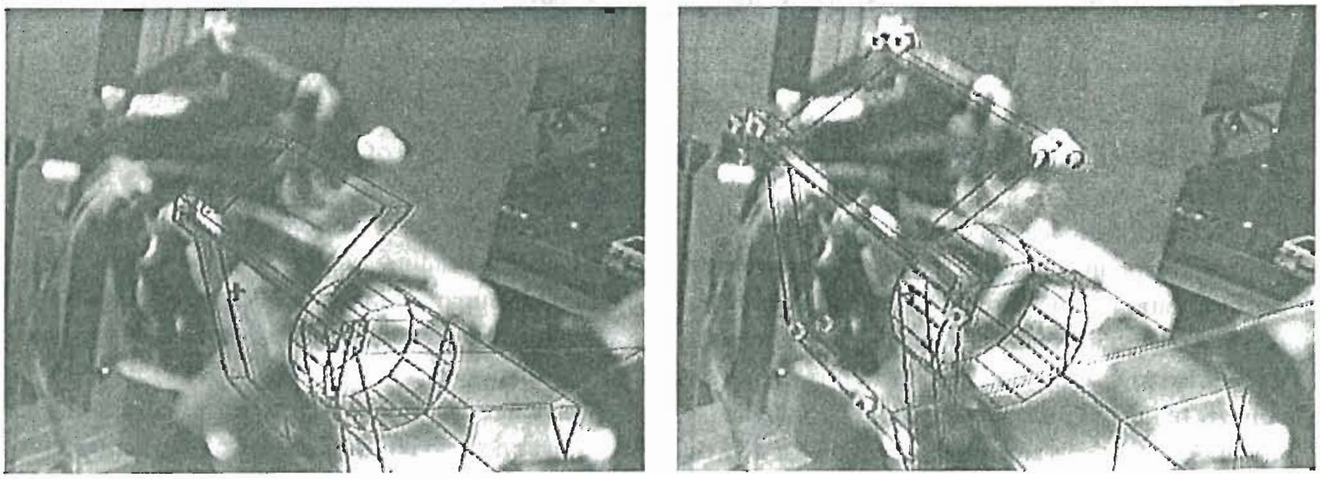

Figure 11. *Superimposed images during calibration. (a) Before calibration. (b) After calibration.*

4.1 Tele-existence Experimental Environment

To test the effectiveness of the control by tele-existence experimentally, we created an experimental environment. The environment model consisted of pipes, a lever, a box, and a ventilating fan. There was a smoke machine to generate smoke in the environment. A lever in the right of the photograph could be rotated to shut off the smoke.

This tele-existence experimental environment consisted of a collection of simple shapes. The environment model described by a model description language was converted to the virtual environment drawing program, which uses surface data, by the conversion program of the model-based calibration system. This environment simulates a small part of a room in a factory as shown in Figure 8. The environment model was displayed by computer graphics as shown in Figure 9. The graphics computer could generate about 12 stereo images every second. The lever to shut off the smoke could also be operated in a virtual environment.

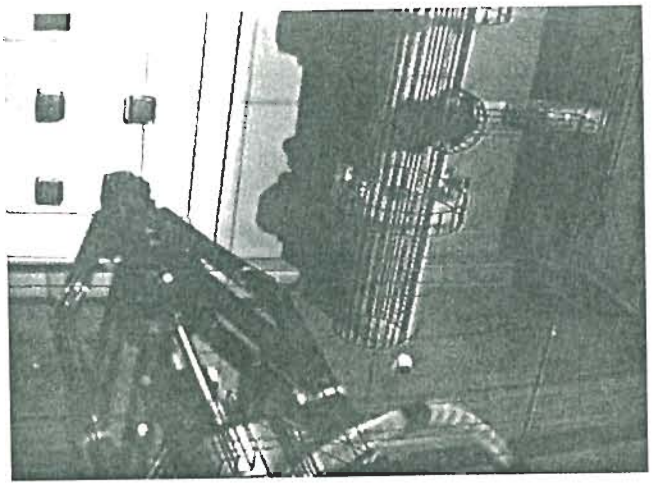

Figure 12. *Results of calibration.*

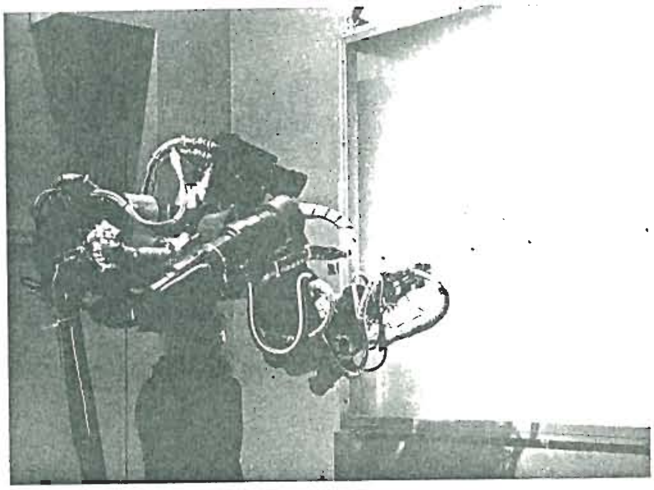

Figure 13. *Operation in poor visibility environment.*

4.2 Calibration Experiment

To test the model-based calibration system, the calibration experiments were conducted. The position and the rotation of the slave robot were sensed by the data from the robot's mobile system. The parameters that needed to be estimated were the errors in the parameters of the mobile objects in the environment model. Stereo images at a resolution of 669 × 453 pixels were used for the calibration. Figure 10a shows the superimposed real and virtual images (wire frame display) of the lever. The distance between the cameras and the lever was about 0.8 m. When the camera was aligned perfectly, the positioning error of a measured point in the three-dimensional space could be estimated from the residual difference of the measured point on the screen. The maximum position errors of the lever were estimated at 4.2 cm in a direction perpendicular to the line of sight of the camera and 16.5 cm in a direction parallel to the line of sight, assuming that the specifications of the stereo camera of the robot were correct. Six parameters, e.g. the 3-D position and 3-D orientation of the experimental environment, were estimated using the calibration system. Twenty-four points on the camera images were used for the estimation. Figure 10b shows the superimposed image after calibration. Small circles in this photograph shows the points of the environment model used for this calibration experiment. The maximum position error of the points on the lever were estimated at 1.5 cm in a direction perpendicular to the line of sight and 2.9 cm in a direction parallel to the line of sight after the calibration. The position accuracy of an image measurement in a direction parallel to the line of sight is usually low. Although stereo images were used, the accuracy was also low.

To reduce the weight of the slave arm, the arm actuators have no zero point. There are offsets on the joint angles that cannot be acquired from the encoders and the offsets must therefore be estimated. Since this arm has 7 DOF, it is difficult to estimate the offsets with one measurement in one attitude. Measurements in 10 different attitudes of the robot arm were conducted. Eighty-four points on the images were used for the estimation. Figure 11a shows the superimposed real and virtual images of the slave robot hand before calibration. The maximum position error of the hand's endpoint was estimated at 6.5 cm in a direction perpendicular to the line of sight and 13.2 cm in a direction parallel to the line of sight. Figure 11b shows an image of the hand after calibration. The maximum position error of the hand's endpoint was estimated at 2.5 cm in a direction perpendicular to the line of sight and 4.2 cm in a direction parallel to the line of sight after the calibration. But the error increased at other attitudes that were not used for the estimation and reached 6.9 cm in a direction perpendicular to the line of sight. Figure 12 shows the real

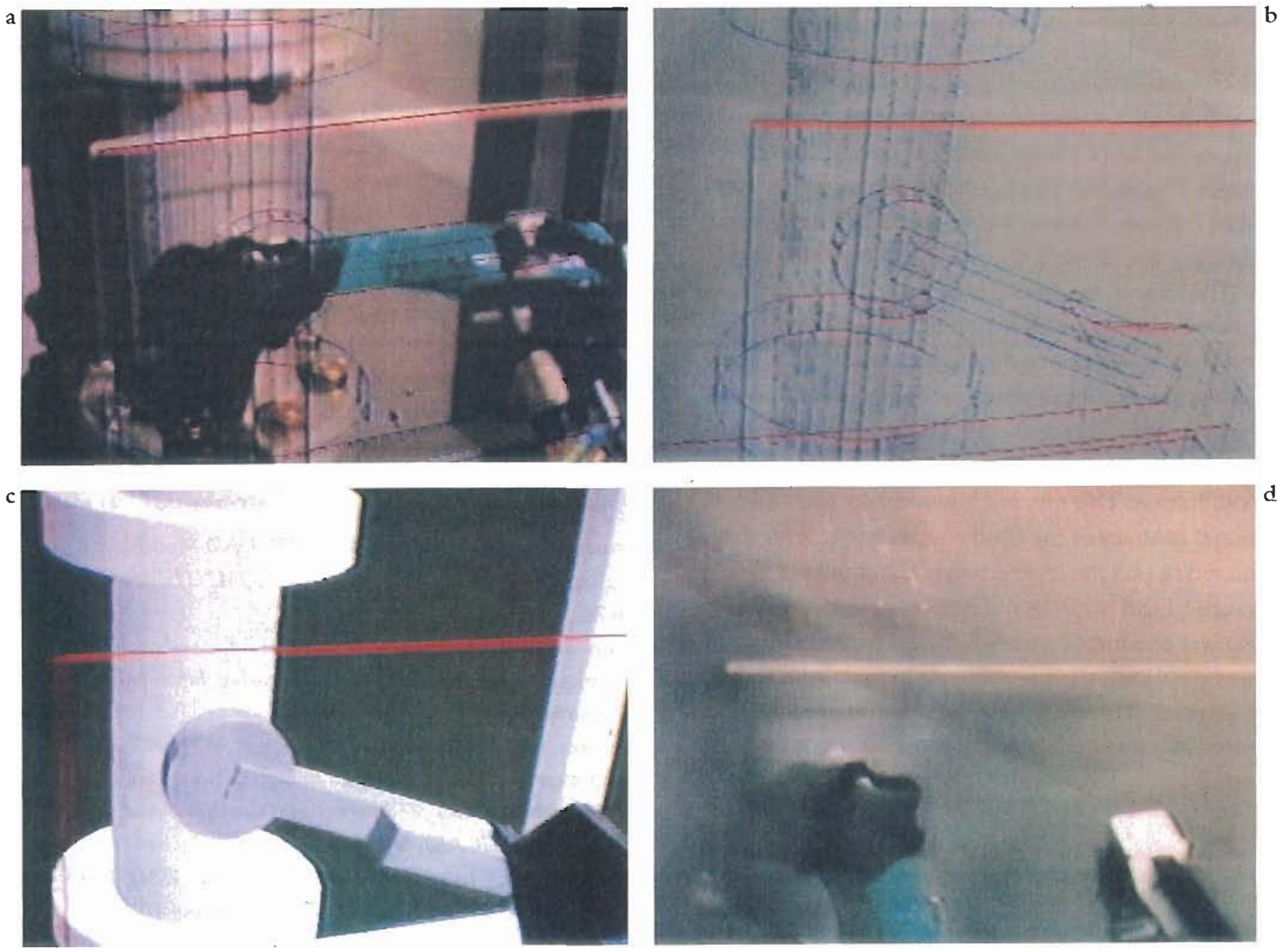

Figure 14. *Displayed images during operation. (a) Camera image of normal environment. (b) Camera image of real environment. (c) Virtual environment. (d) Result of operation.*

image and the updated virtual environment after calibration.

4.3 Operation in Poor Visibility Environment

To test the extended tele-existence system, we conducted an experiment operating the slave robot in a poor visibility environment.

In the tele-existence experimental environment, the smoke machine generated smoke and the slave robot's sense of sight became useless. The task of pulling a lever down, which requires a comparatively low degree of precision, was successfully performed by the slave robot. For this task, the desired impedance characteristics in Eq. (2) were:

$$M = 6I \text{ (kg)} \tag{19}$$

$$B = 100I \text{ (Ns/m)} \tag{20}$$

$$K = 50I \text{ (N/m)} \tag{21}$$

where I is the identity matrix. A photograph of the robot working in a poor visibility environment is shown in Figure 13.

Figure 14 shows images displayed during the operation. Figure 14a shows the camera image overlaid by a wire frame model of the environment during normal operation. Figure 14b shows actual camera images overlaid with the wire frame model of the virtual environment during operation in the poor visibility environment. The lever in the smoke is almost completely obscured. Figure 14c is an image of the virtual environment seen by the operator during the operation. Figure 14d shows the end result when the smoke was removed.

The lever was successfully pulled down. Impedance control could compensate for errors that still remained after calibration. This task is a low accuracy task. The positional accuracy of the hand relative to the lever that is required to pull the lever down is about 6.0 cm in both vertical and horizontal directions. Hence, the operation was conducted successfully. To perform more precise operations, the environment model needs to be more accurate. Therefore more parameters need to be estimated and the intelligence of the slave robot must be improved.

5 Conclusion

To conduct an operation in poor visibility environments, we proposed an extended tele-existence system using virtual reality. We developed the model-based calibration system to superimpose a virtual environment on a real environment precisely. To confirm the performance of the experimental extended tele-existence system, we successfully performed an experimental operation in a poor visibility environment. This system has only limited capabilities at present. However, if the slave robot has a range sensor that can work in poor visibility environments, the system functions adequately in such environments.

References

Akin, D. L., Minsky, M. L., Thiel, E. D., & Kurtman, C. R. (1983). Space application of automation, robotics and machine intelligence systems (ARAMIS)—phase II. NASA Contractor Report 3734.

Bejczy, A. K., & Kim, W. S. (1990). Predictive displays and shared compliance control for time-delayed telemanipulation. *Proceedings of IEEE International Workshop on Intelligent Robotics and Systems, 1,* 407–412.

Bejczy, A. K., Kim, W. S., & Venema, S. V. (1990). The Phantom robot: Predictive displays for teleoperation with time delays. *Proceedings of the International Conference on Robotics and Automation,* 546–511.

Brooks, R. A. (1981). Symbolic reasoning among 3-D models and 2-D images. *Artificial Intelligence, 17,* 285–348.

Fisher, S. S., McGreevy, M., Humphries, J., & Roinett, W. (1986). Virtual environment display systems. *Proceedings of the 1986 Workshop on Interactive 3-D Graphics, 77–87.*

Gunnarsson, K. T., & Prinz, F. B. (1987). CAD Model-based localization of parts in manufacturing. *COMPUTER, 20*(8), 66–74.

Hashimoto, T., & Sheridan, T. B. (1986). Effects of predictive information in teleoperation with time delay. *Japan Journal of Ergonomies, 22*(2).

Hightower, J. D., Spain, E. H., & Bowles, R. W. (1987). Telepresence: A hybrid approach to high-performance robots. *Proceedings of the '87 International Conference on Advanced Robotics (ICAR),* 563–573.

Hogan, N. (1985). Impedance control Part I–III. *ASME Journal of Dynamic Systems, Measurement, and Control, 101*(1), 1–24.

Hogan, N. (1987). Stable execution of contact task using impedance control, *Proceedings of IEEE International Conference on Robotics and Automation,* 1047–1057.

Inoue, Y., Tachi, S., & Arai, H. (1992). A method for impedance control of a master-slave manipulation system. *Journal of the Robotics Society of Japan, 10*(4), 490–500 (in Japanese).

Lowe, D. G. (1980). Solving for the parameters of object models from image descriptions. *Proceedings of ARPA Image Understanding Workshop,* College Park, MD, 121–127.

Lowe, D. G. (1985). *Perceptual organization and visual recognition.* Boston: Kulwer Academic Publishers.

Lowe, D. G. (1987). Three-dimensional object recognition from single two-dimensional images. *Artificial Intelligence, 31*(3), 355–395.

Machida, K., Toda, Y., & Iwata, T. (1990). Graphics-simulator-augmented teleoperation system for space applications. *Journal of Spacecraft and Rockets, 27*(1), 64–69.

Marquardt, D. W. (1963). An algorithm for least square estimation of nonlinear parameters. *Journal of Society of Industrial Applied Mathematics, 11.*

Mason, M. T. (1981). Compliance and force control for computer controlled manipulator. *IEEE Transaction on Systems, Man and Cybernetics,* 418–432.

Noyes, M. V., & Sheridan, T. B. (1984). A novel predictor for telemanipulation through a time delay. *Proceedings of the 20th Annual Conference on Manual Control.*

Oyama, E., & Tachi, S. (1990). Model-based image measurement system. *JASME Papers (C), 56*(521), 109–115 (in Japanese).

Park, J. H., & Sheridan, T. B. (1991). Supervisory teleoperation control using computer graphics. *Proceedings of the IEEE International Conference on Robotics and Automation,* 493–498.

Salisbury, J. K. (1980). Active stiffness control of a manipulator in Cartesian coordinates. *Proceedings of the IEEE International Conference on Decision and Control, 102,* 95.

Sheridan, T. B. (1982). Supervisory control: Problems, theory and experiment for undersea remote systems. MIT Man-Machine Systems Labrador Report.

Stark, L., Kim, W. S., et al. (1987). Telerobotics: Display, control, and communication problems. *IEEE Journal of Robotics and Automation, RA-3*(1), 67–75.

Tachi, S., & Abe, M. (1982). Tele-existence (I)—Design of visual display. *Proceedings of SICE'82 (The Society of Instrument and Control Engineers),* 157–168 (in Japanese).

Tachi, S., & Arai, H. (1985). Tele-existence (II)—Three dimensional display with sensation of presence. *Proceedings of the '85 International Conference on Advanced Robotics (ICAR),* 345–352.

Tachi, S., Arai, H., & Maeda, T. (1988). Tele-existence simulator with artificial reality. *Proceedings of the IEEE International Workshop on Intelligent Robotics and Systems (IROS'88).*

Tachi, S., Arai, H., & Maeda, T. (1990). Tele-existence master slave system for remote manipulation. *IEEE International Workshop on Intelligent Robotics and Systems (IROS'90).*

Tachi, S., Arai, H., Maeda, T., Oyama, E., Tsunemoto, N., & Inoue, Y. (1991). Tele-existence in real world and virtual world. *Fifth International Conference on Advanced Robotics (ICAR),* 193–198.

Tachi, S., & Sakaki, T. (1990). Impedance controlled master slave system for tele-existence. *Proceedings of the First International Symposium on Measurement and Control in Robotics.*

Tachi, S., Tanie, K., & Komoriya, K. (1981). A control method for manipulator with sensory information display. Japanese Patent No. 1348263, Jan. 14.

Tachi, S., Tanie, K., Komoriya, K., & Kaneko K. (1984). Tele-existence (I)—Design and evaluation of a visual display with sensation of presence. *Proceedings of the 5th Symposium on Theory and Practice of Robots and Manipulators (RoManSy 84),* 245–254.

Tanabe, T., Ohyama, E., & Koyama, H. (1985). Model based vision system for autonomous teleoperated spacecraft. *American Astronautical Society/Japanese Rocket Society Joint International Symposium,* AAS 85-661.

Tanabe, T., Ohyama, E., & Koyama, H. (1986). Visual information processing system for autonomous teleoperated spacecraft. *15th International Symposium on Space Technology and Science.*